UHASSELT
KNOWLEDGE IN ACTION

Maastricht University

Faculty of Medicine and Life Sciences
School for Life Sciences
Master of Biomedical Sciences

Master's thesis

Epithelial Cell Rests of Malassez as Endothelial and Osteoclast Regulators in the Periodontium

Mai Hoang Ngoc Phuong

Thesis presented in fulfillment of the requirements for the degree of Master of Biomedical Sciences, specialization Molecular Mechanisms in Health and Disease

SUPERVISOR :
Prof. dr. Ivo LAMBRICHTS

CO-SUPERVISOR :
dr. Florian HERMANS

2024
2025

Transnational University Limburg is a unique collaboration of two universities in two countries: the University of Hasselt and Maastricht University.

UHASSELT
KNOWLEDGE IN ACTION

www.uhasselt.be
Universiteit Hasselt
Campus Hasselt:
Martelarenlaan 42 | 3500 Hasselt
Campus Diepenbeek:
Agoralaan Gebouw D | 3590 Diepenbeek

UHASSELT
KNOWLEDGE IN ACTION

Maastricht University

Faculty of Medicine and Life Sciences
School for Life Sciences
Master of Biomedical Sciences

Master's thesis

Epithelial Cell Rests of Malassez as Endothelial and Osteoclast Regulators in the Periodontium

Mai Hoang Ngoc Phuong

Thesis presented in fulfillment of the requirements for the degree of Master of Biomedical Sciences, specialization Molecular Mechanisms in Health and Disease

SUPERVISOR :
Prof. dr. Ivo LAMBRICHTS

CO-SUPERVISOR :
dr. Florian HERMANS

UHASSELT *Senior internship- 2nd master BMW*

Epithelial Cell Rests of Malassez as Endothelial and Osteoclast Regulators in the Periodontium*

Mai Hoang Ngoc Phuong[1], Steffie Hasevoets[1], Pieter Ruytinx[2], Annelies Bronckaers[1], Ivo Lambrichts[1] and Florian Hermans[1]

[1]Group of Cardiology and Organ Systems (COS), Biomedical Research Institute, Hasselt University, Campus Diepenbeek, Agoralaan Gebouw C - B-3590 Diepenbeek
[2]Department of Immunology and Infection, Biomedical Research Institute, Hasselt University, Campus Diepenbeek, Agoralaan Gebouw C - B-3590 Diepenbeek

*Running title: Epithelial Cell Rests of Malassez Regulatory Role

To whom correspondence should be addressed:
Florian Hermans, Tel: +32(11) 26 83 39; Email: florian.hermans@uhasselt.be
Ivo Lambrichts, Tel: +32 (11) 26 92 45; Email: ivo.lambrichts@uhasselt.be

Keywords: *Periodontitis, periodontal ligament regeneration, ERM's secretome, tooth organoid, functional validation*

ABSTRACT

Periodontitis is a major cause of tooth loss and significantly impacts the quality of life through chronic inflammation and destruction of tooth-supportive tissues. Current regenerative treatments offer limited success. Epithelial cell rests of Malassez (ERM), found in the periodontal ligament and dental follicle, have emerged as important players in maintaining periodontal tissue homeostasis and regeneration. Our previous data and other studies show that ERM expresses pro-angiogenic (VEGF, IL-6) and osteoclast-regulatory (CCL2) factors, suggesting a role in signaling. This study aims to functionally validate whether conditioned medium from ERM-derived tooth organoids (ERM-TO CM) enhances osteoclast and endothelial cell differentiation. Expression of VEGF, IL-6, CCL2, and VEGFRs were evaluated by immunohistochemistry in human periodontal tissue or by ELISA of ERM-TO CM. The angiogenic potential was assessed using tube formation assays in dental pulp stem cells (DPSCs) and human microvascular endothelial cells (HMEC-1). Osteoclast differentiation from peripheral blood mononuclear cells (PBMCs) was assessed by TRAP staining and bone resorption assays. ERM and nearby blood vessels expressed VEGF, VEGFR1, VEGFR2, and CCR2. ELISA confirmed the presence of VEGF, IL-6, and CCL2 in ERM-TO CM. ERM-TO CM promoted endothelial differentiation and tube formation in DPSCs but had no significant effect on tube formation in HMEC-1. It also enhanced PBMC-derived osteoclast differentiation in pilot experiments, although further optimization is required. These findings provide functional support for ERM as a signaling hub within periodontal tissue, with secreted factors that may contribute to angiogenesis and bone remodeling in the context of regenerative therapies.

INTRODUCTION

Periodontal diseases, including periodontitis, are among the leading oral health conditions contributing significantly to the global burden of disease, as measured by disability-adjusted life years (DALYs) in the Global Burden of Disease Study 2021 (1). Additionally, it was estimated over 1 billion people (12.5%) worldwide suffered from severe periodontitis, and the number is expected to increase to 1.5 billion by 2050. Periodontitis is characterized by the accumulation of dental plaques (a sticky film of bacteria formed on the teeth), causing chronic inflammation. As the disease progresses, the prolonged inflammation causes damage to the periodontium, a structure composed of gingiva (the soft tissue surrounding the teeth), alveolar bone, periodontal ligament (PDL), and cementum (**see Figure 1**) (2,3). This further leads to bacteria pocket formation, bone resorption, and eventually tooth loss if left untreated (4). Periodontitis often progresses

silently, without noticeable symptoms, until significant damage has occurred. As the leading cause of periodontium damage, this disease significantly diminishes patients' chewing ability, self-confidence, esthetics, and quality of life (5). In Europe, periodontal disease was estimated to cause a loss of 158.64 billion euros in 2018 due to direct costs associated with treatment and indirect costs related to loss of productivity (6).

Conventional periodontitis therapies focus on removing infection sources and reshaping gingiva and alveolar bone to reduce pocket depth (scaling, root planning, and respective periodontal surgery) (7,8). However, these methods are unable to regenerate the tissue damaged by chronic inflammation, thus leading to a shift toward development of regenerative periodontal treatment strategies. Currently, bone grafting and guided tissue/bone regeneration techniques have been widely introduced to the clinic. These methods provide a barrier to prevent gingival outgrowth into the alveolar bone while allowing the progenitor and stem cells to regenerate the tooth-supportive tissues (4,9). To further promote healing, biological agents like purified recombinant human platelet-derived growth factor-BB (PDGF-BB) and enamel matrix derivatives have been used in combination with bone graft or guided tissue/bone regeneration method (10). Although these methods have shown promising results in enhancing treatment efficacy, complete periodontium regeneration remains elusive due to the complexity of tissue regeneration and the need for coordinated cellular and molecular interactions (8,11). Thus, better understanding of cell-cell communication during periodontal development and homeostasis might open new avenues to develop novel therapeutic approaches in dentistry. Being part of the periodontium, PDL is a complex soft connective tissue essential for anchoring the tooth to the alveolar bone (12). Epithelial cell rests of Malassez (ERM) are epithelial stem cells present in the PDL or dental follicle (DF; a transient structure present during tooth development, which eventually regresses to form PDL after root formation). Developmentally, ERM are remnants of Hertwig's epithelial root sheath, which is an essential signaling hub guiding root formation (13). Though typically quiescent, ERM can be activated and proliferate under inflammatory conditions (14). Furthermore, rat ERM have been shown to aid in periodontal regeneration in response to periodontal disease (15,16). For instance, ERM are believed to contribute to the restoration of periodontal fibroblasts and cementoblasts through epithelial-to-mesenchymal transition (EMT). Moreover, ERM have been shown to secrete prostaglandins and enamel proteins, which in turn stimulate the release of bone matrix proteins—such as BMP-2, osteopontin, osteoprotegerin, and sialoprotein—thereby promoting cementum formation and periodontal tissue repair (14,17,18).

Importantly, during development and homeostasis, ERM are thought to play an essential role in maintaining the periodontal space, preventing root resorption (breakdown of dental root structure) and dentoalveolar ankylosis (i.e., fusion of the tooth root to alveolar bone due to loss of PDL and replacement of soft connective tissue by mineralized bone tissue). One possible explanation for this function is that ERM can modulate coordinated activity of osteoblasts and osteoclasts (17,18). When this balance is disturbed, e.g. during periodontitis, osteoclasts become hyperactive, leading to bone erosion and, eventually, tooth loss (2,17). Moreover, previous research has shown a close association of nerve fibers with the ERM, which was also similar to our previous finding, suggesting that ERM are involved in coordinating and maintaining periodontal innervation (18). In addition, ERM are thought to control the correct positioning of periodontal vasculature in the periodontal space (19).

Thus, a key mechanism underlying ERM's diverse properties has been associated with their signaling profile. Previous research identified several osteoclast-stimulating factors secreted by ERM, including epidermal growth factors and their receptors, bone-resorptive agents, and prostaglandins (17). These factors contribute to preventing bone invasion and maintenance of PDL space. ERM have also been shown to express enamel matrix proteins, bone matrix proteins, and bone morphogenic protein-2, aiding in promoting osteogenesis for periodontal and cementum repair

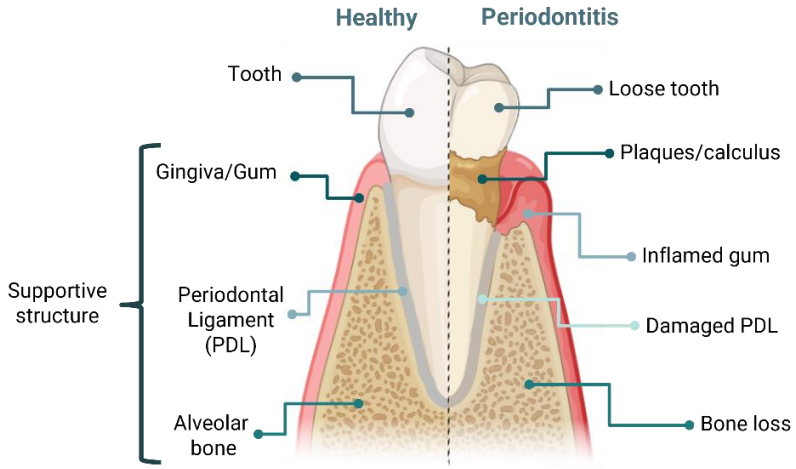

Fig. 1 – Structure of the tooth in normal condition and under periodontitis

(20,21). The expression of different factors known to both promote bone resorption as well as stimulate osteogenesis indicates the complex role of ERM in maintaining the delicate balance between osteoclasts and osteoblasts in the periodontal space. Neuropeptides, indicative of the notion that ERM support periodontal innervation, and inflammatory cytokines (e.g., interleukin (IL)-1α, IL-6, IL-8) were also found to be expressed by ERM (17,18). Furthermore, using primary culture of ERM-derived epithelial cells, the profile of ERM's signaling factors has been further expanded with a significant amount of cytokines, growth factors, chemokines, and their related proteins, especially revealing the presence of urokinase-type plasminogen activator receptor (uPAR), and vascular endothelial growth factor (VEGF-A, referred herein as VEGF), both well-known pro-angiogenic factors (22,23). The expression of these angiogenesis factors may explain the putative role of ERM in regulating the positioning of periodontal vasculature (19). However, the findings in the study by Oshima *et al.* (2008) were limited by the fact that the screened cytokines have not been functionally validated (i.e. by examining their functional interactions between ERM and other niche cells). Additionally, the 2D cell culture model used for cytokine screening has not been well characterized and might share some differences with the *in situ* environment. Therefore, a better-representing model, as well as further screening and functional validation of the ERM secretome, are necessary to confirm these findings.

In recent decades, with the advancement in understanding the biology of extracellular matrix and improvement in cell suspension cultures, organoid culture has been developed. Organoids are defined as self-organizing 3D *in vitro* structures that more closely resemble *in vivo* organs in terms of tissue architecture and functionality, than traditional 2D cell models (24). Organoids can be derived from pluripotent stem cells or adult stem cells, including from diseased donors while maintaining patient characteristics *in vitro* (25). With the above benefits, there has been a shift in the recent decade toward using organoid models to uncover human biology and development, disease mechanisms, and serve as models for drug screening (24,25). Previously, our research group successfully established and characterized human ERM-derived tooth organoids (ERM-TO). The established ERM-TO closely mimics human ERM in terms of expressed markers (cytokeratin-14, E-cadherin, SOX2), their capability to undergo EMT and produce enamel matrix proteins, as well as ERM-mirroring signaling profiles (Unpublished work-Dr. F. Hermans, 23,24)). Our preliminary data is in line with the observation of Oshima *et al.* (2008): revealing the presence of angiogenic (e.g. IL6, uPAR, VEGFA), neurogenic (e.g. βNGF), immunoregulatory (e.g. IL4, GCP2), and osteoclast stimulatory (e.g. TIMP1, chemokine (C-C) ligand-2 (CCL2)) proteins in the conditioned medium of ERM-TO (ERM-TO CM; unpublished data). Moreover, their expression (e.g., *VEGFA*, *CCL2*) has been confirmed in native ERM using single-cell transcriptomics and RNA *in situ* hybridization.

Nevertheless, the functional relevance of these secreted factors requires further validation.

Hence, the present study aims to functionally validate the angiogenic and osteoregulatory human ERM signaling axes by combining ERM-TO-secreted factors with *in vitro* differentiation, tube formation, and bone resorption assay. Our hypothesis is that signaling factors secreted by ERM-TO can promote endothelial and osteoclast differentiation and functionality *in vitro*. The results from this study are anticipated to offer new fundamental insights into ERM's role as signaling hubs, as well as novel perspectives on how signaling factors may be utilized to enhance the integration process in tooth implantation and periodontal tissue engineering.

EXPERIMENTAL PROCEDURES

Organoid culture and conditioned medium collection

Predominantly unerupted third molars were collected from adolescent patients (16-22 years old) at Ziekenhuis Oost-Limburg (ZOL, Genk, Belgium) with written informed consent and ethical approval from the medical ethical committee of Hasselt University (protocol 13/104U). The DF or PDL was isolated and dissociated from the third molar to establish ERM-TO, as previously developed by our group (18,27). In general, dissociated DF cell suspension was mixed with growth factor-reduced Matrigel (Corning) at a ratio of 30:70 and seeded at 20,000 cells per 20 µL drop in a 48 or 96-well plate (Greiner). Tooth organoid medium (TOM; Table S1) was then added to the wells containing solidified gel domes. 10 µM ROCK inhibitor Y-27632 (Merck Millipore) was supplemented in the culture medium during the first 2 days of seeding or passaging to prevent anoikis. Organoids were cultured at 37°C in 1.9% CO_2, and the medium was refreshed every 2-3 days. After every 10–14 days, ERM-TOs were passaged, and the CM was collected during passages 1-4. The TO-derived medium was collected 48-72h after refreshing the culture medium once organoids reached a diameter of 50-100 µm. The collected medium was stored at -80°C for ELISA or subsequent functional assays.

Glucose measurements

To normalize differences in growth rate (and thus the amount of secreted factors) between organoids from different donors, glucose (mg/dL) was measured in collected CMs and the negative control mediums using a GlucCell glucose meter and GlucCell test strips (Esco Bioengineering) Ratiometric normalization was performed relative to the appropriate negative control medium (see further).

Cell culture

Dental pulp stem cells (DPSCs) from the unerupted third molars were isolated using the explant outgrowth method, as previously described (29,30). Isolated DPSCs were cultured in α-Minimum Essential Medium (α-MEM, Capricorn Scientific) containing 20% fetal calf serum (FCS, Biowest), 1% penicillin-streptomycin (P/S, Gibco), along with 1% L-glutamine (Gibco). DPSCs were passaged twice for stabilization before usage in tube formation assays. HMEC-1 cells were kindly provided by the Centre of Disease Control and Prevention (Atlanta, GA). The cells were cultured in MCDB-131 (Gibco) supplemented with 10% FCS, 10 mM L-glutamine, 100 U/mL P/S, 10 ng/mL EGF (Gibco), and 1 µg/mL hydrocortisone (Alfa Aesar). Cells were incubated at 37°C in 5% CO2, and the medium was refreshed every 2-3 days.

Tube formation assay

Tube formation assay was performed in flat bottom 96-well plates (Sarstedt) coated with 50 µL growth factor-reduced Matrigel (Corning) per well 1-2h before cell seeding. To remove bubbles, the plates were placed on ice for 15-20 minutes before solidifying in a 37°C cell incubator. DPSCs were seeded into the coated plate at 2,000 cells per well in culture medium (D0). The next day (D1), the medium was switched to the following four conditions: (1) serum-free defined medium (SFDM, Table S2) containing 1% P/S, 1% L-glutamine, and 5% FCS as a negative control (basal medium), (2) basal medium supplemented with 20 ng/mL platelet-derived growth factor BB (PDGF-BB, R&D Systems), and 25 ng/mL basic fibroblast growth factor (bFGF, R&D Systems) as a positive control (endothelial differentiation medium), (3) TOM, and (4) diluted CMs (26,31). The CMs were diluted in the negative control medium according

to the glucose measurement for normalization of the difference in secreted factors (**Normalized V_{CM} (mL) = V_{final} x (glucose CM/glucose negative medium)**). Cells were incubated at 37°C, and 1.9% CO_2 with medium refreshes every 2-3 days. Images were recorded on D7; the total length, number of tubes, and average length formed by DPSC-derived endothelial cells were measured by ImageJ. A minimum length threshold of 30 µm was applied during the measurements.

For HMEC-1 tube formation, a 96-well Matrigel-coated plate was prepared, similar to that of DPSCs. After that, the cells were seeded at 20,000 cells/well directly in four different conditions: (1) SFDM with 1% P/S, 1% L-glutamine (full SFDM) as positive control, (2) full SFDM supplemented with 10% FCS as negative control, (3) TOM, (4) internal control 'a' (ICa), (5) internal control 'b' (ICb), (6) diluted CMs. The CMs were diluted in the negative control medium for normalization to glucose level, as mentioned previously. Internal control 'a' and 'b' were TOM diluted in negative control with 0.66 and 0.18 ratios, respectively (according to the highest and lowest dilution required for CMs). Cells were cultured at 37°C, and 1.9% CO_2 for 24h with images taken at 6h and 24h. The obtained images were quantified by ImageJ Angiogenesis Analyzer (32).

Osteoclast from peripheral blood monocyte differentiation

Peripheral blood was collected from healthy donors under informed consent, and PBMCs were isolated using the Ficoll gradient centrifugation method (Ficoll, Tebubio). Isolated PBMCs were seeded either onto 96-well plates for adherence and differentiation assays, or onto dentine slices for functional resorption analysis. Seeded cells were incubated in α-MEM supplemented with 1% FCS (Gibco) and 1% P/S at 37°C in 5% CO_2 for 3h to allow adherence. After incubation, non-adherent cells were removed by washing twice with phosphate-buffered saline (PBS). Images of adhered cells were acquired via Primovert inverted cell culture microscope (ZEISS), and quantification was performed using color threshold analysis in ImageJ. For osteoclast differentiation, adhered PBMCs were cultured under specific induction conditions: (1) a-MEM supplemented with 1% P/S, and 10% FCS (basel medium) as negative control, (2) basel medium supplemented with 1 ng/mL TGF-B1, 30 ng/mL M-CSF, 1 ng/mL or 10 ng/mL RANKL as positive control, (3) SFDM diluted in basel medium with 1:1 ratio, (4) ERM-TO CM diluted approximately 1:1 in basal medium to normalize glucose levels, and supplemented with 1 ng/mL TGF-β1, 30 ng/mL M-CSF, and either 1 ng/mL or 10 ng/mL RANKL. Medium was changed every 2–3 days. Cells were maintained at 37°C in a humidified atmosphere with 5% CO_2.

TRAP assay

To assess osteoclast formation from PBMC, TRAP assay was performed on D14. The cells were first fixed with 4% paraformaldehyde (PFA, Sigma-Aldrich) for 20 mins at 4°C. Then, cells were washed with PBS two times. TRAP staining solution was prepared according to the Leukocyte Acid Phosphatase Kit (Sigma-Aldrich), and cells were stained for 15 minutes in the dark. The reaction was stopped by washing with PBS one time, and pictures were recorded using a Primovert inverted cell culture microscope (ZEISS). Osteoclasts are defined as TRAP-positive cells with more than three nuclei (33).

Bone resorption assay

To assess bone resorption *in vitro,* PBMCs were seeded onto dentine slices and differentiated into osteoclasts over a 14-day period, as described above. TRAP staining was performed to confirm osteoclast formation on the dentine surface. Following staining, cells were removed from the slices by gently wiping with tissue. Resorption pits were then visualized by briefly immersing the dentine slices in thionine methylene blue solution. Images of the resorption pits were captured using a Primovert inverted cell culture microscope (ZEISS).

ELISA assay

The concentration of IL6, VEGF, and CCL2 in collected CMs was assessed using ELISA. As a negative control, medium collected from wells containing only Matrigel droplets incubated for 48-72h (similarly to the time for collecting medium from organoids wells after refreshing) was used. ELISA was performed according to the manufacturer's instructions (human IL-6 ELISA MAX™ Deluxe Set (BioLegend), human VEGF

ELISA MAX™ Deluxe Set (BioLegend), and ELISA MAX™ Deluxe Set human MCP-I/CCL2 (BioLegend)). The results obtained were normalized for glucose measurements according to the following formula.

Normalized concentration (pg/mL) = obtained concentration x (glucose patient sample/glucose Matrigel sample)

Histochemical and immunohistochemistry staining (IHC)

An archival slide of human mandibular bone tissue with Masson's Trichrome staining was kindly provided by Prof. Dr. Ivo Lambrichts. For histological and IHC staining, primary DF or PDL tissues were fixed with 4% PFA at room temperature (RT) for 24h. Then, tissues were embedded in paraffin and cut into 4 µm thick sections. Deparaffinization and rehydration were performed using xylene and a graded series of ethanol. The deparaffinized sections were either subjected to hematoxylin and eosin staining or IHC staining. For IHC, antigen retrieval (10 mM Sodium citrate, 0.05% Tween 20, pH 6.0) was performed at 95°C for 30 mins. Next, endogenous peroxidase activities were blocked using 3% H_2O_2 for 25 mins at RT and nonspecific binding sites were blocked with serum-free protein block (DAKO) at RT for 20 mins. The primary antibody was incubated overnight at 4°C, and the secondary antibody for 30 mins. 3,3'-Diaminobenzidine (DAB; DAKO, K3468) staining was performed according to the manufacturer's instructions. DAB-stained sections were then counterstained with Gill's Hematoxylin for 3 mins and blued in xxx ammonium water before dehydration and mounting (EcoMount, Biocare Medical).

Dual immunohistochemical staining for TP63 and VEGF was performed using DAB and ImmPACT® VIP (Vector Laboratories) substrates. The general procedure followed the protocol described above, with both primary antibodies incubated simultaneously overnight at 4°C. On the following day, sequential detection was performed: TP63 was incubated and visualized first using the DAB substrate, followed by a mild quenching step with 0.3% H_2O_2 to inactivate residual peroxidase activity. VEGF was then incubated and visualized using the VIP substrate.

TP63/CD31 dual immunohistochemical staining was performed using a sequential HRP-based protocol adapted from TP63/VEGF staining. TP63 primary antibody was applied first, followed by the corresponding HRP-conjugated secondary antibody and color development with DAB. A quenching step with 0.3% H_2O_2 and blocking with serum-free protein block was then performed. CD31 primary antibody was subsequently applied, followed by a second HRP-conjugated secondary antibody and color development with VIP. The antibodies used for immunohistochemistry staining are listed in **Table 1**.

Table 1 – Primary and secondary antibodies

Primary Antibody		
Mouse Anti-VGFR2	1/200	Santa Cruz, SC-6251
Rabbit Anti-VEGFR1	1/100	Proteintech,13687-I-AP
Mouse Anti-CCR2	1/200	Biotechne, NBP2-35334
Mouse Anti- VEGF	1/100	Biotechne, NB100-664
Rabbit Anti-CD31	1/100	Bethyl Laboratories, IHC-00055
Rabbit Anti-TP63	1/1000	Abcam, ab124762
Secondary Antibody		
HRP-Goat Anti-Mouse	1/100	Agilent Technologies, P0447
HRP-Goat Anti-Rabbit	1/100	Dako, P0449

Statistical analysis

Statistical analysis was performed using GraphPad Prism 10.4.2. All data were presented as mean ± standard error of the mean (SEM). Statistical difference was determined by mixed model ANOVA with p=0.05. All experiments were performed with ≥ 3 independent biological experiments (unless otherwise indicated).

RESULTS

ERM role in angiogenesis and osteoclasia through its expression profile

To understand the role of ERM in regulating PDL niche homeostasis, archival Trichrome Masson's stained human jaw tissue from a periodontitis patient was re-imaged to explore tissue structure and morphological changes surrounding ERM (**Figure 2A**). Within the sample of the periodontitis patient, it was clear to distinguish between undamaged regions (i.e., nicely organized and structured presence of PDL,

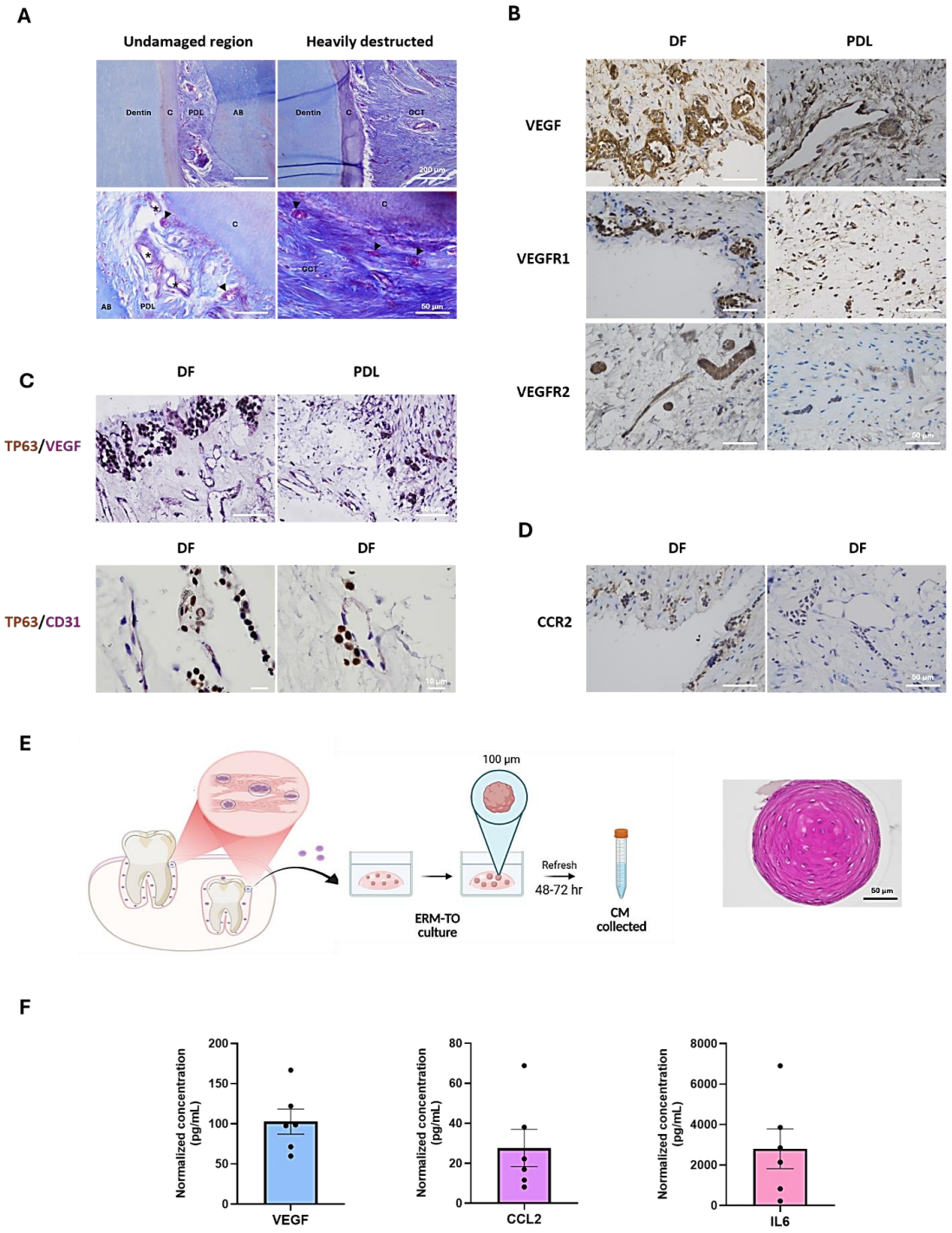

Fig. 2. Presence of angiogenic and osteoclastic factors in ERM tissue and ERM-TO CM. (A) Human jaw tissue from a periodontitis patient (n=1), stained with Masson's Trichrome. Structures labeled: Cementum (C), Alveolar Bone (AB), Periodontal Ligament (PDL), Gingival Connective Tissue (GCT), Epithelial Rests of Malassez (ERM; arrowheads), and blood vessels (*). **(B)** DAB IHC staining of VEGF, VEGFR1, and VEGFR2 in human DF and PDL tissues (n=3). **(C)** mIHC co-labeling of TP63 (DAB) with VEGF or CD31 (VIP) in DF (n=3) and PDL (n=2). **(D)** DAB IHC staining of CCR2 in human DF and PDL tissues (n=3). **(E)** Schematic of ERM-TO CM collection process. **(F)** ELISA quantification of VEGF, CCL2, and IL6 (n=6) in ERM-TO CM. Each dot represents an individual biological replicate. Results were expressed as mean ± SEM

alveolar bone) and regions of severe periodontitis (heavily destructed alveolar bone, loss of PDL tissue, and invasion of gingival connective tissue).

No clear differences in the number of ERMs between the regions were observed, however, undamaged regions were more vascularized, with small blood vessels situated close to ERM clusters. This suggests that in undamaged regions, ERM might have a role in regulating PDL vasculature. In contrast, the periodontitis-affected regions exhibited fewer blood vessels in proximity to ERM, implying a possible disruption of this regulatory function, potentially mediated by inflammation-induced alterations in the ERM's secretome.

To examine the potential involvement of ERM in regulating blood vessel position, the presence of pro-angiogenic factor VEGF and its receptors VEGFR1 and VEGFR2 was assessed in DF and PDL tissues via immunohistochemistry (**Figure 2B**). VEGF is a key angiogenesis factor that not only serves as a survival factor but also a growth-promoting factor for endothelial cells (34). This growth factor functions by binding to its receptors VEGFR1 and VEGFR2. In human DF and PDL tissue, VEGF was detected in endothelial cells, ERM, and the surrounding fibroblasts. Interestingly, not just endothelial cells but also ERM expressed both VEGFR1 and VEGFR2. Additionally, VEGFR1 appeared more
widely expressed in periodontal stromal cells as well.

Additionally, in the human DF tissue stained for the presence of VEGF, VEGFR1, and VEGFR2, it was observed that there were positive cell clusters that resemble both the morphology of ERMs and blood vessels. Hence, further co-stain for both ERM markers and blood vessel markers was performed to clarify their relationship (**Figure 2C**). Co-staining of TP63 (an epithelial stem cell marker expressed in ERM) and VEGF (angiogenesis marker in ERM and endothelial cells) or CD31 (specific endothelial cell marker) with mIHC confirmed the intimate association of ERM with blood vessels (3,35,36). This further supports the hypothesis that ERM may regulate blood vessel formation and homeostasis.

Previous research has indicated a potential osteoclast-stimulating effect of ERM (17). We previously identified the presence of CCL2 in ERM and the CM of ERM-TO (unpublished work, Dr. F. Hermans). CCL2 is a chemokine that has been reported to be upregulated in gingival periodontitis and plays an important role in monocyte recruitment and subsequent osteoclast formation (37,38). To detect the targets of CCL2 activity in ERM tissue, immunohistochemistry against C-C chemokine receptor type 2 (CCR2), a CCL2 receptor, was performed (**Figure 2D**). CCR2 is known to be expressed on the surface of monocytes/macrophages (39,40). With the staining, it is expected to review attracted monocytes close to ERM tissue. The result confirmed the expression of CCR2 in single cells around ERM; nevertheless, their monocytes/macrophage identity required further confirmation using CD14/CD68 staining. Interestingly, CCR2 was also expressed in endothelial cells and ERM. Notably, CCR2 expressions in both ERM and blood vessels appeared low and exhibited variability across the stained samples.

Finally, the identification of VEGF, CCL2, and IL-6 in the secretome of ERM-TO CM using ELISA supports the ERM as one of the sources that secrets signaling factors contributing to angiogenesis and osteoclast regulation in the periodontium (**Figure 2F**). The glucose concentration used for normalization across conditions is provided in **Table S3**.

ERM-TO CMs increase differentiation and tube formation of DPSC but not mature endothelial cells

Tube formation assay is one of the most widely used *in vitro* assays to model angiogenesis. Hence, for further functional validation of the effect of signaling factors present in ERM-TO CMs effect on angiogenesis, a tube formation assay using two different endothelial cell models (DPSCs and HMEC-1) was performed (**Figures 3-4**). Previously, Zhang et al., 2022 established the tube formation *in vitro* model using DPSCs (31). Given their dental origin, we expect that using this model can provide more niche-relevant insights into not just tube formation but also the differentiation process of DPSCs to endothelial cells under the

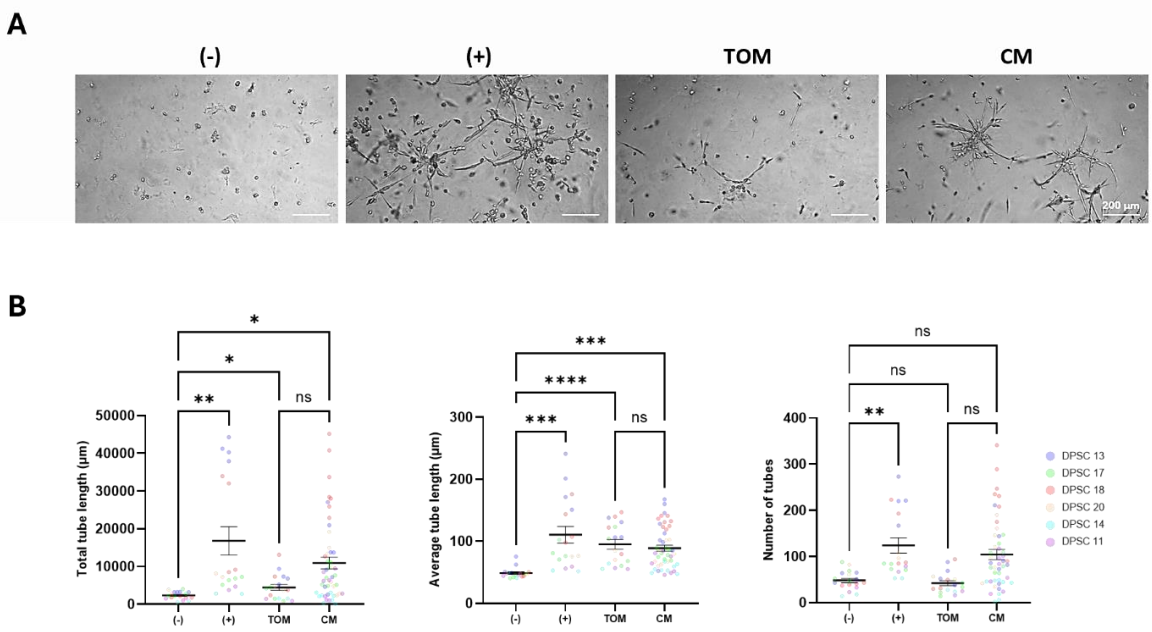

Fig. 3 – ERM-TO CM modulates DPSC-EC differentiation and tube formation. (A) Endothelial cell differentiation and tube formation of DPSCs in different conditions on D7. (-): negative control, (+): positive control, TOM: tooth organoid medium, CM: ERM-TO CM diluted in (-) medium for glucose normalization. **(B)** Quantification of tube formation using ImageJ, the statistical analysis was performed using mixed model ANOVA (n=6). Results were expressed as mean ± SEM, * $p < 0.05$, ** $p < 0.01$, *** $p < 0.001$, **** $p < 0.0001$.

effect of ERM-TO CM. Compared to the negative, positive, and internal control (TOM, the medium for culturing TO), ERM-TO CM elicited enhanced endothelial tube formation of DPSC (**Figure 3A**). Quantification of the formed tubes showed enhanced total length and total number of tubes in ERM-TO CM compared with (-), (+), and TOM.

Interestingly, although TOM induced limited numbers of tubes, the average length of those formed was similar to those induced by ERM-TO CM and the positive control. Moreover, the biological variance (of DPSC and CM derived from different donors) was quite large (**Figure S.1**). Even so, our data suggests that ERM-TO CM can enhance the endothelial differentiation and tube formation of DPSCs.

Although the tube formation capacity of DPSCs could offer good insight into the effects of ERM-TO conditioned medium (CM) on endothelial differentiation and angiogenic potential, confirmation was pursued using a second, more widely utilized endothelial cell model. HMEC-1, an immortalized human microvascular endothelial cell line, was selected due to its established reliability and stability *in vitro* tube formation assays (41,42) (**Figure 4**). The ERM-TO CM showed a slight enhancement in tube formation compared to the negative control and positive control. However, TOM alone had a significant impact on tube formation, highlighting the need for additional internal controls to account for its effects. Furthermore, a key difference from previously published HMEC-1 tube formation protocols was the presence of fetal calf serum (FCS), which, in our system, appeared to inhibit tube formation compared to serum-free conditions. As a result, 0% FCS in SFDM was used as a negative control and 10% FCS in SFDM as a positive control. To account for the potential effects of FCS and TOM dilution on HMEC-1 tube formation, additional internal controls were included (**Figure 4A & S2**). After comparing the ERM-TO CM group with internal controls, quantification results did not show much difference between the groups. In conclusion, in terms of mature endothelial cells, the ERM-TO CM did not

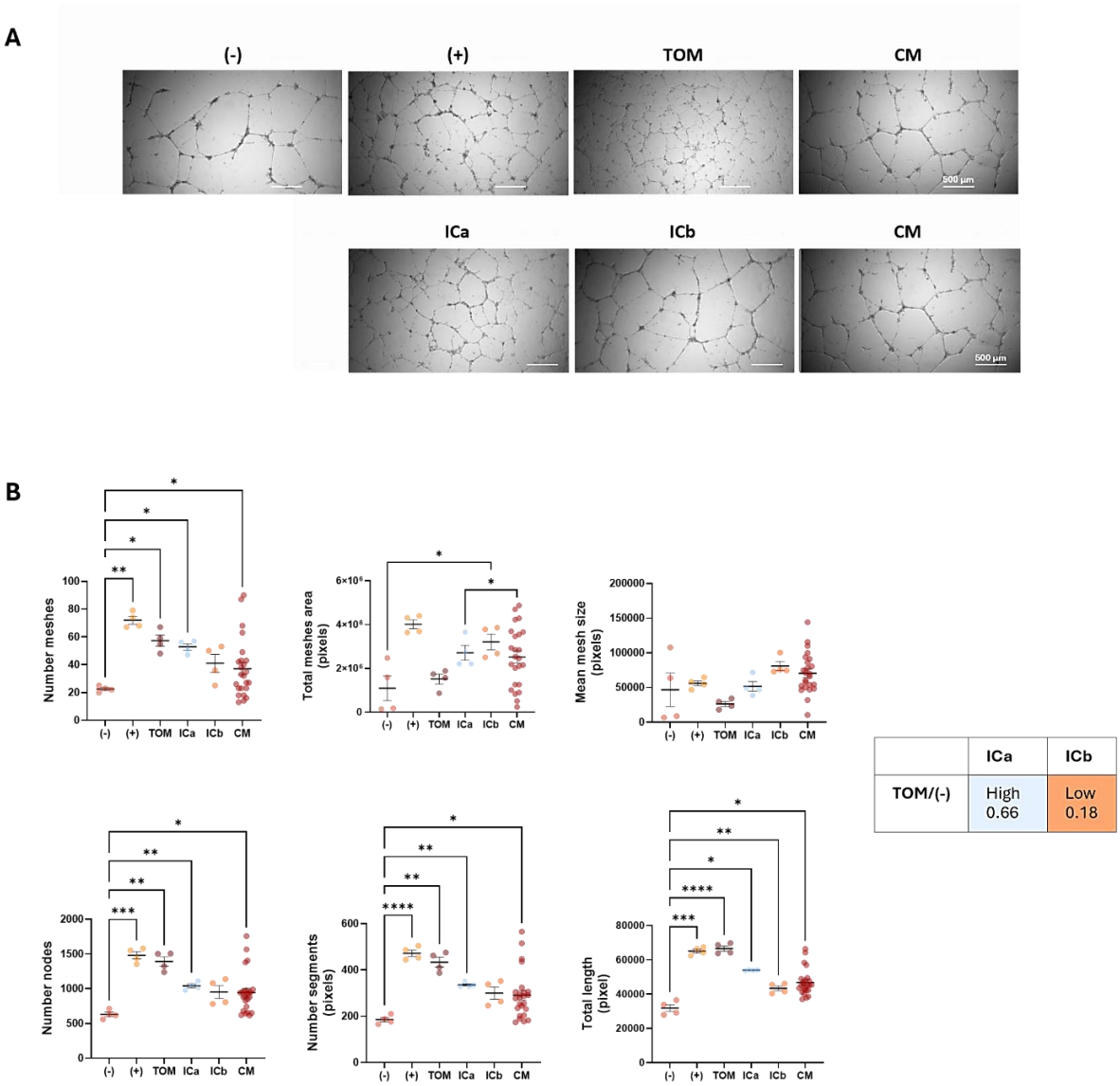

	ICa	ICb
TOM/(-)	High 0.66	Low 0.18

Fig. 4 – **ERM-TO CM effect in HMEC-1 tube formation. (A)** Endothelial cell differentiation and tube formation of HMEC-1 in different conditions at 24h. (-): negative control, (+): positive control, TOM: tooth organoid medium, ICa : internal control 'a', ICb: internal control 'b', CM: ERM-TO CM diluted in (-) medium for glucose normalization **(B)** Quantification of tube formation using ImageJ, the statistical analysis was performed using mixed model ANOVA (n=1). Results were expressed as mean ± SEM, * $p < 0.05$, ** $p < 0.01$, *** $p < 0.001$, **** $p < 0.0001$.

have a significant effect that can distinguish CM-specific responses from the non-specific effects of TOM.

ERM-TO CMs increase osteoclast differentiation rate however not consistent

Osteoclasts are derived from the monocyte-macrophage lineage and differentiate from hematopoietic precursor cells, including monocytes, through a complex, multi-step process (43). Monocytes are well known for their adherence to endothelial cells, a critical step that facilitates their migration to sites of inflammation or injury, where they differentiate into macrophages or participate in tissue repair. *In vitro*, the adherence of monocytes to plastic surfaces has been used as a model to study their adhesion

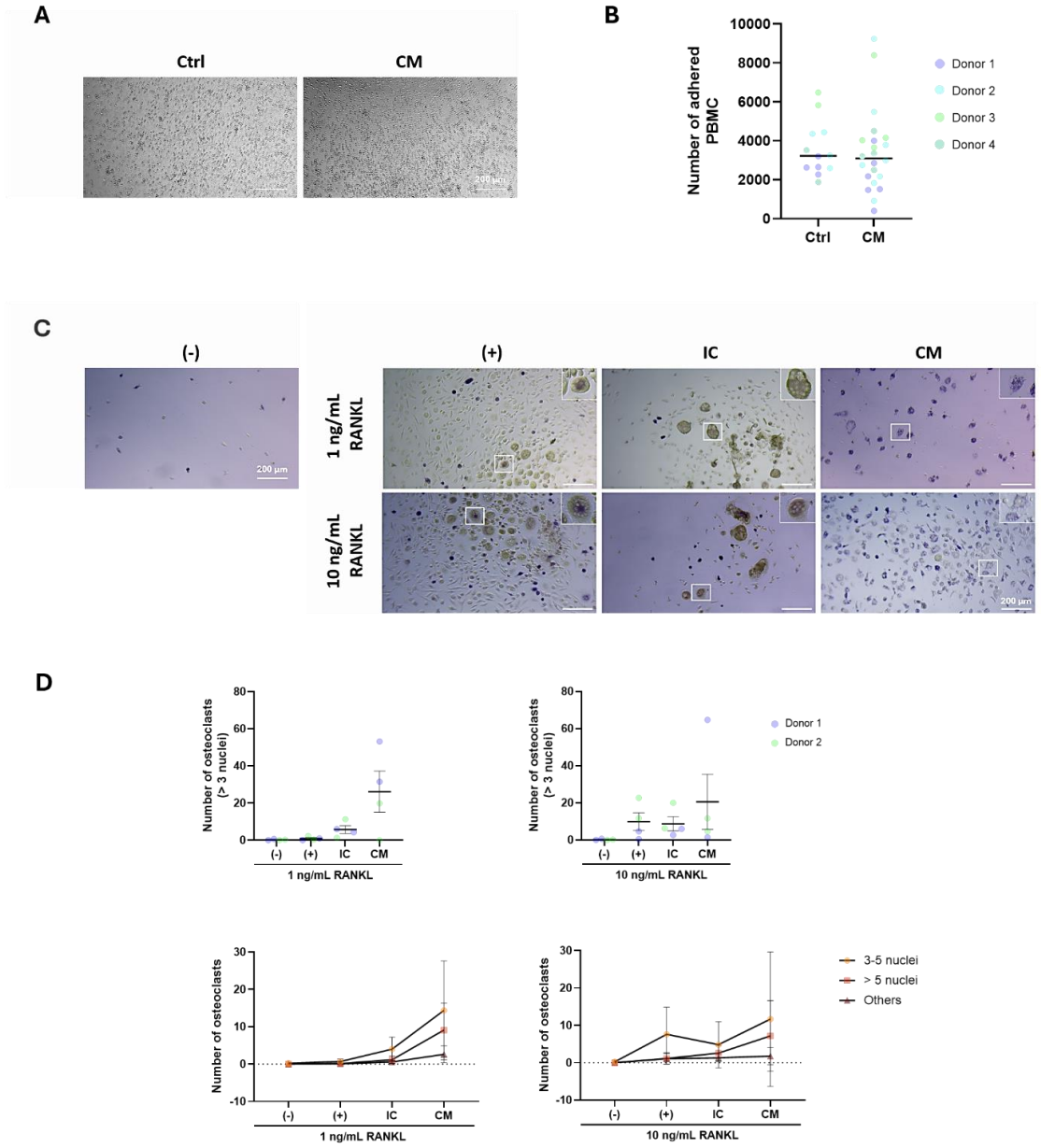

Fig. 5– ERM-TO CM effect on osteoclast differentiation. (A) Adherence of PBMC under the effect of ERM-TO CM (n=4). Ctrl: aMEM supplemented with 1% FCS, and 1% P/S as control medium, CM: ERM-TO CM diluted in control medium **(B)** Semi-automated quantification of adhered human PBMC by ImageJ. **(C)** TRAP assay to assess the osteoclast differentiation of human PBMC in different conditions on D14 (n=2). (-) negative control, (+) positive control, (IC) internal control where TOM was diluted in (-) with similar ratio as CM, (CM): ERM-TO CM diluted in (-) for glucose normalization. **(D)** Quantification of the TRAP positive osteoclasts with more than 3 nuclei in ImageJ. Data was analyzed by mixed model ANOVA. Results were expressed as mean ± SEM, * $p < 0.05$, ** $p < 0.01$, *** $p < 0.001$, **** $p < 0.0001$.

behavior (44,45). Previous studies have shown that monocyte adhesion is an important prerequisite for subsequent osteoclast differentiation and activation (46). In this experiment, we investigated the effect of ERM-TO CM on monocyte adhesion using a plastic surface as the *in vitro* model (**Figure 5A&B**). Compared to the control condition, ERM-TO CM preserved the adhesive properties of

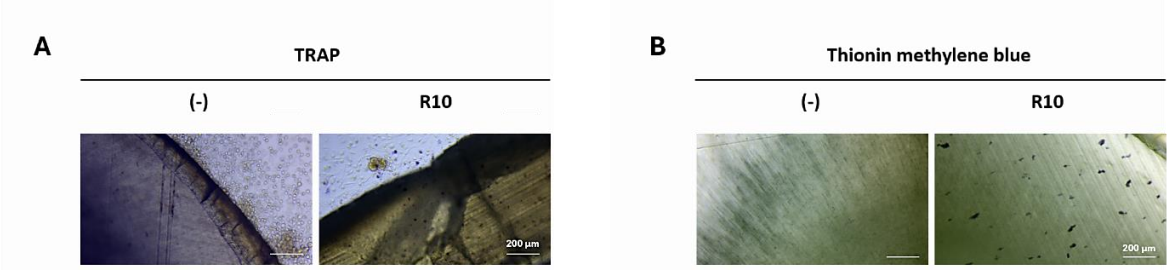

Fig. 6 – Bone resorption assay optimization. (A) TRAP staining to assess multinucleated osteoclasts on dentine slice on D14. **(B)** Thionine methylene blue to assess the resorption pit on dentine slice (n=2).

PBMCs but did not significantly enhance adhesion. Furthermore, considerable variability was observed among donors, indicating that the effect of CM on monocyte adhesion may be donor-dependent and might require wider population investigation.

To evaluate the effect of ERM-TO CM on osteoclast differentiation from PBMCs, PBMCs were seeded into 96-well plates and treated with CM in the presence of transforming growth factor beta-1 (TGF-β1), macrophage colony-stimulating factor (M-CSF) and varying concentrations of soluble receptor activator of nuclear factor κB ligand (RANKL, 1 ng/mL and 10 ng/mL), the key hematopoietic factors regulating osteoclastogenesis. Direct differentiation of PBMCs under ERM-TO CM alone, without M-CSF, TGF-β1 and RANKL, was not performed due to the detrimental effects of TOM, which severely compromised the survival of PBMC-derived osteoclasts (**Figure S3**). Addition of low (1 ng/mL) and high (10 ng/mL) RANKL concentrations was performed to reveal ERM-TO CM-specific effects while avoiding saturation, where high RANKL levels might mask any additional osteoclastogenic influence of the CM. Given that tartrate-resistant acid phosphatase (TRAP) expression and multinucleation are well-established markers of osteoclast commitment and maturation, TRAP staining was performed to identify mature osteoclasts, defined as TRAP-positive cells containing more than three nuclei (43,47,48).

Morphologically, osteoclasts differentiated in the presence of ERM-TO CM exhibited increased multinucleation compared to controls, indicating a potential pro-osteoclastogenic effect (**Figure 5C**). However, the nuclear morphology of these cells appeared atypical, with a higher nucleus-to-cytoplasm ratio than observed in the positive control or internal control (IC) groups. These alterations suggest that the CM may influence not only the extent of multinucleation but also the structural integrity of the resulting osteoclasts. Additionally, it is noted that there was a great variance in the effect of ERM-TO CM on osteoclast differentiation (**Figure S4**).

Quantitative analysis revealed a higher number of TRAP-positive multinucleated osteoclasts (≥3 nuclei) in both RANKL1 and RANKL10 conditions when CM was applied (**Figure 5D**). Interestingly, CM under RANKL1 conditions induced a greater osteoclastogenic effect than under RANKL10, implying that CM may have a more pronounced impact under sub-threshold RANKL stimulation. Furthermore, CM treatment also led to an increased proportion of osteoclasts containing more than five nuclei. The degree of multinucleation has been suggested to correlate with the upregulated expression of osteoclastic genes and is associated with enhanced bone resorption activity (49). Nevertheless, the morphology of osteoclasts differentiated in the presence of CM differed from that of the control groups. Further investigation into cellular markers and functional characteristics is required to better understand their maturation status and whether they have enhanced bone resorption activity.

As a first step to further investigate the bone resorption activity of osteoclasts differentiated in the presence of ERM-TO CM, a bone resorption assay was optimized using both negative (without M-CSF and RANKL) and positive (with M-CSF and RANKL) control conditions (**Figure 6**). TRAP staining was used to evaluate the presence of mature osteoclasts on dentine slices, while thionine

methylene blue staining was employed to visualize resorption pits. Although mature osteoclasts were not clearly observed, distinct and quantifiable resorption pits were evident in the positive control group. These findings indicate that, in future experiments, osteoclasts differentiated under ERM-TO CM conditions can be cultured directly on dentine slices to assess their bone resorption capacity.

In conclusion, although no statistically significant effects were observed, the data suggest a potential positive influence of ERM-TO CM on osteoclast differentiation, particularly under conditions of low RANKL stimulation. The observed morphological differences and increased multinucleation indicate that ERM-TO CM may modulate not only osteoclast formation but also cellular characteristics (e.g. cell morphology), highlighting the need for further investigation using additional osteoclast maturation markers and functional assays across a broader range of donor samples.

DISCUSSION

ERM role in angiogenesis and osteoclasia through its expression profile

In this study, we found that ERM in human periodontal tissue expresses the angiogenic factor VEGF. The presence of VEGF suggests that ERM may serve as a local source of this growth factor, potentially contributing to the regulation of blood vessel formation and endothelial cell migration. It has been known that VEGF exerts its effects primarily through binding to its receptors on endothelial cells. VEGFR2 is recognized as the principal mediator of VEGF-driven angiogenesis, while VEGFR1 is often described as a "decoy" receptor that can inhibit VEGF activity by sequestering it away from VEGFR2 (34,50,51). Therefore, ERM may influence endothelial cell behavior and vascular formation through the secretion of VEGF and its interaction with these receptors on endothelial cells.

Interestingly, ERM was also found to express both VEGFR1 and VEGFR2. Previous studies have shown that, in addition to endothelial cells, these receptors are also expressed on hematopoietic stem cells (HSCs), lung epithelial cells (specifically alveolar type II cells), and various tumor cells (34,52,53). In HSCs, both VEGFR1 and VEGFR2 contribute to a VEGF-dependent autocrine signaling loop that promotes cell survival through a phosphoinositide 3-kinase (PI3K)-dependent pathway. The expression of both VEGF receptors in ERM may similarly indicate the presence of an autocrine mechanism that supports stem cell survival or maintenance. Furthermore, high VEGFR1 expression in DPSCs has been associated with enhanced endothelial differentiation potential (54). This raises the possibility that ERM may also possess a greater capacity for endothelial differentiation, which could be relevant for applications in vascular tissue engineering. Whether ERM can undergo such differentiation *in vivo* remains an open and intriguing question.

In addition to pro-angiogenic factors, this study also revealed that both ERM and blood vessels within human periodontal tissue exhibited inconsistent expression of CCR2. Previous studies have reported CCR2 expression in human umbilical vein endothelial cells (HUVECs), although protein levels are generally low under basal conditions and become upregulated in response to inflammation (55). Since the periodontal tissues analyzed in this study were obtained from healthy donors, the low or inconsistent CCR2 expression observed in both ERM, and blood vessels may reflect a non-inflamed physiological state. Moreover, expression of CCR2 on endothelial cells (e.g., HUVEC) was found to aid in their migration toward damaged tissue areas during wound repair (55). Besides endothelial cells, an HSCs subset in mice was also found to express CCR2, which aids in their homing capability to the site of inflammation (56). Furthermore, genetic modification to generate CCR2 overexpression in mesenchymal stem cells (MSCs) has been reported to enhance MSC migration toward damaged liver sites (57). Together, these findings suggest that ERM may also possess migratory capabilities, potentially enabling them to home to areas of inflammation

and participate in immune signaling or tissue regeneration processes.

The detection of VEGF, CCL2, and IL-6 in ERM-TO further supports the role of ERM in regulating not only angiogenesis but also monocyte recruitment, potentially enhancing osteoclast formation through the CCL2/CCR2 signaling axis. Notably, the CCL2/CCR2 pathway has been implicated not only in monocyte chemotaxis but also in promoting vasculature (58,59). Collectively, these findings suggest a multifaceted role for ERM in coordinating blood vessel formation for better immune cell recruitment, potentially facilitating osteoclast differentiation. In addition, the presence of IL-6, an important mediator of inflammation, confirms a possible role for ERM in immune modulation.

ERM-TO CMs increase differentiation and tube formation of DPSC but not mature endothelial cells

Our findings revealed that ERM-TO CM enhanced endothelial cell differentiation and tube formation from DPSCs. Notably, there was variance between the ERM-TO CM collected from different donors. Future research might want to combine the collected ERM-TO CMs into one batch before using for minimizing this variation effect.

This study also found that ERM-TO CM did not significantly increase tube formation in HMEC-1 cells. This lack of response may be attributed to the nature of HMEC-1 as a more mature endothelial cell line, which potentially expresses a broader array or higher sensitivity of receptors responsive to various angiogenic components present in TOM, such as fibroblast growth factor 2. As a result, these factors may have confounded the interpretation of ERM-TO CM-specific effects by masking or overlapping with its angiogenic signals. Furthermore, it should be noted that instead of using high serum concentration (10%) for positive control, we used 0% instead. Because 10% FCS combining with our basel medium SFDM released an inhibition effect on tubes formed. This effect can be due to the higher presence of glucose in our basel medium (~140 mg/dL) in compared with a-MEM (~100 mg/dL). Previous research has noted an effect of higher glucose in 10% serum medium released a growth inhibiting effect while high glucose in 0.5% serum medium stimulated cell growth on bovine carotid artery endothelial cells (60).

Collectively, these findings suggest that the ERM-TO secretome primarily supports the initiation of blood vessel formation, including aspects of vascular positioning and regeneration, rather than promoting endothelial maturation or vessel stabilization.

ERM-TO CMs increase osteoclast differentiation rate however not consistent

Our findings demonstrated that ERM-TO CM did not have a statistically significant effect on the adherence of monocyte-derived cells from PBMCs to plastic surfaces, compared to the control condition. This lack of significance may be attributed to donor variability or differences in the composition of the collected CM. Given that CCL2 is a chemokine known to mediate the recruitment of CCR2+ monocytes, future studies should explore the potential of ERM-TO CM to attract osteoclast precursors rather than focusing solely on adhesion. A suitable model for this investigation could be the human monocyte transendothelial migration *in vitro* assay (61).

Additionally, our pilot results indicate that the presence of ERM-TO CM in cultures with 1 ng/mL RANKL led to a marked but statistically insignificant increase in osteoclast formation from PBMCs. The lack of statistical significance may be attributed to small sample size (n=2), high variability within the dataset, likely due to donor-to-donor differences. One possible explanation is that some donor-derived cells may rapidly consume osteoclast-regulatory factors present in the CM, depleting these signals before the differentiation process can be completed. Oshima et al. (2008) reported that ERM expresses M-CSF, which may support our finding that ERM-TO CM enhances osteoclast formation (22). Therefore, future studies should consider analyzing both

RANKL and M-CSF levels in the ERM-TO secretome and native ERM (e.g. IHC) to better understand ERM's role in osteoclastogenesis and clarify the underlying mechanisms.

Additionally, it is noted that although ERM-TO CM enhances the number of osteoclasts formed, the morphology of the formed osteoclasts is quite different from that of the control group in terms of nuclei numbers and nuclei/cytoplasm ratio. Future research should perform DAPI staining after TRAP staining to better confirm all the vacuole like structures are nuclei. Additionally, other markers of maturation like the formation of F-actin ring, and expression of osteoclast markers (e.g. cathepsin K, integrin β3, CD51/*ITGAV*) should be addressed to better characterize the maturation state of the obtained osteoclasts (33,62,63). The functional capacity of osteoclasts generated under ERM-TO CM conditions also remains to be determined and should be addressed in future studies.

Our initial optimization of the bone resorption assay using dentine slices successfully produced clear and quantifiable resorption pits. This established protocol can serve as a foundation for future studies investigating the effect of ERM-TO CM on the bone resorptive activity of differentiated osteoclasts. However, it should be noted that the dentine slices used in this study (~300–400 µm thick) limited the visualization of TRAP-stained osteoclasts. To improve cellular imaging and identification, future experiments may consider using thinner dentine sections (e.g., 100–200 µm) to facilitate clearer observation of TRAP-positive osteoclasts.

Throughout this study, substantial variability was observed, largely due to differences in donor-derived ERM-TO CM. To address this limitation, future research should consider pooling all collected CM into a single large batch and normalizing for key factors such as glucose concentration, VEGF, and CCR2 levels to reduce inter-batch variation. Furthermore, variability in the results may also arise from the interference of lymphocytes which was not thoroughly eliminated after the PBMCs adherence and washing step. Isolation of $CD14^+$ monocytes from PBMCs using magnetic-activated cell sorting (MACS) would provide a more specific and enriched precursor population, leading to the formation of a more homogeneous and consistent osteoclast population (33,64). Additionally, osteoclast quantification is a labor-intensive process, which can limit the scalability of the study and restrict analysis across larger sample sizes. Future experiments could benefit from the integration of automated image analysis tools, such as the "Artificial Intelligence for Image-Based Identification of Osteoclasts and Assessment of Their Maturation" approach, to enable more rapid, objective, and scalable quantification. This would not only improve reliability but also allow for the analysis of larger sample populations (65)

CONCLUSION

In summary, our results provide functional evidence supporting the role of ERM-TO CM in promoting angiogenesis, particularly in the processes of development and regeneration, rather than in vascular maturation and stabilization. Our pilot study on the effects of ERM-TO CM on osteoclast regulation also yielded promising findings, indicating enhanced osteoclast differentiation. However, further investigations are necessary to optimize experimental conditions, increase sample size, and comprehensively assess additional markers and bone resorption activity in the differentiated osteoclasts. Collectively, these findings support the potential role of ERM as a signaling hub that regulates both angiogenesis and osteoclast-related signaling pathways.

REFERENCES

1. Bernabe E, Marcenes W, Abdulkader RS, Abreu LG, Afzal S, Alhalaiqa FN, et al. Trends in the global, regional, and national burden of oral conditions from 1990 to 2021: a systematic analysis for the Global Burden of Disease Study 2021. The Lancet [Internet]. 2025 Feb 27 [cited 2025 Mar 6];0(0). Available from: https://www.thelancet.com/journals/lancet/article/PIIS0140-6736(24)02811-3/fulltext
2. Kinane DF, Stathopoulou PG, Papapanou PN. Periodontal diseases. Nat Rev Dis Primers. 2017 Jun 22;3(1):1–14.
3. Seo BM, Song IS, Um S, Lee JH. Chapter 22 - Periodontal Ligament Stem Cells. In: Vishwakarma A, Sharpe P, Shi S, Ramalingam M, editors. Stem Cell Biology and Tissue Engineering in Dental Sciences [Internet]. Boston: Academic Press; 2015 [cited 2024 Jul 17]. p. 291–6. Available from: https://www.sciencedirect.com/science/article/pii/B9780123971579000242
4. Bosshardt DD, Stadlinger B, Terheyden H. Cell-to-cell communication – periodontal regeneration. Clinical Oral Implants Research. 2015;26(3):229–39.
5. Wang X, Chen J, Tian W. Strategies of cell and cell-free therapies for periodontal regeneration: the state of the art. Stem Cell Res Ther. 2022 Dec 27;13(1):536.
6. Botelho J, Machado V, Leira Y, Proença L, Chambrone L, Mendes JJ. Economic burden of periodontitis in the United States and Europe: An updated estimation. Journal of Periodontology. 2022;93(3):373–9.
7. Graziani F, Karapetsa D, Alonso B, Herrera D. Nonsurgical and surgical treatment of periodontitis: how many options for one disease? Periodontology 2000. 2017;75(1):152–88.
8. Kwon T, Lamster IB, Levin L. Current Concepts in the Management of Periodontitis. International Dental Journal. 2021 Dec 1;71(6):462–76.
9. Lee HS, Byun SH, Cho SW, Yang BE. Past, Present, and Future of Regeneration Therapy in Oral and Periodontal Tissue: A Review. Applied Sciences. 2019 Jan;9(6):1046.
10. Suárez-López del Amo F, Monje A, Padial-Molina M, Tang Z, Wang HL. Biologic Agents for Periodontal Regeneration and Implant Site Development. Biomed Res Int. 2015;2015:957518.
11. De Lauretis A, Øvrebø Ø, Romandini M, Lyngstadaas SP, Rossi F, Haugen HJ. From Basic Science to Clinical Practice: A Review of Current Periodontal/Mucogingival Regenerative Biomaterials. Advanced Science. 2024;11(17):2308848.
12. Kaku M, Yamauchi M. Mechano-regulation of collagen biosynthesis in periodontal ligament. Journal of Prosthodontic Research. 2014 Oct 1;58(4):193–207.
13. Jeong JK, Kim TH, Choi H, Cho ES. Impaired breakdown of Herwig's epithelial root sheath disturbs tooth root development. Developmental Dynamics. 2024;253(4):423–34.
14. Davis EM. A Review of the Epithelial Cell Rests of Malassez on the Bicentennial of Their Description. Journal of Veterinary Dentistry. 2018;35:290–8.
15. Helal M, Alsherif A. The ameliorating role of epithelial cell rests of Malassez in the alleviation of experimentally-induced periodontitis in rats. Archives of oral biology. 2023;149:105658.
16. Pulitano Manisagian GE, Benedí D, Goya JA, Mandalunis PM. Study of epithelial rests of Malassez in an experimental periodontitis model. Acta Odontol Latinoam. 2018 Dec;31(3):131–7.
17. Silva BS e, Fagundes N, Nogueira BCL, Valladares J, Normando D, Lima RR. Epithelial rests of Malassez: from latent cells to active participation in orthodontic movement. Dental Press Journal of Orthodontics. 2017;22:119–25.
18. Xiong J, Gronthos S, Bartold P. Role of the epithelial cell rests of Malassez in the development, maintenance and regeneration of periodontal ligament tissues. Periodontology 2000. 2013;63 1:217–33.

19. Kat PSP, Sampson WJ, Wilson DF, Wiebkin OW. Distribution of the epithelial rests of Malassez and their relationship to blood vessels of the periodontal ligament during rat tooth development. Aust Orthod J. 2003 Nov;19(2):77–86.
20. Hasegawa N, Kawaguchi H, Ogawa T, Uchida T, Kurihara H. Immunohistochemical characteristics of epithelial cell rests of Malassez during cementum repair. J Periodontal Res. 2003 Feb;38(1):51–6.
21. Yamawaki K, Matsuzaka K, Kokubu E, Inoue T. Effects of epidermal growth factor and/or nerve growth factor on Malassez's epithelial rest cells in vitro: expression of mRNA for osteopontin, bone morphogenetic protein 2 and vascular endothelial growth factor. J Periodontal Res. 2010 Jun;45(3):421–7.
22. Ohshima M, Yamaguchi Y, Micke P, Abiko Y, Otsuka K. In Vitro Characterization of the Cytokine Profile of the Epithelial Cell Rests of Malassez. Journal of Periodontology. 2008;79(5):912–9.
23. Bifulco K, Longanesi-Cattani I, Gala M, DI Carluccio G, Masucci MT, Pavone V, et al. The soluble form of urokinase receptor promotes angiogenesis through its Ser^{88}-Arg-Ser-Arg-Tyr^{92} chemotactic sequence. J Thromb Haemost. 2010 Dec;8(12):2789–99.
24. Rossi G, Manfrin A, Lutolf MP. Progress and potential in organoid research. Nat Rev Genet. 2018 Nov;19(11):671–87.
25. Heydari Z, Moeinvaziri F, Agarwal T, Pooyan P, Shpichka A, Maiti TK, et al. Organoids: a novel modality in disease modeling. Bio-des Manuf. 2021 Dec 1;4(4):689–716.
26. Hemeryck L, Hermans F, Chappell J, Kobayashi H, Lambrechts D, Lambrichts I, et al. Organoids from human tooth showing epithelial stemness phenotype and differentiation potential. Cellular and Molecular Life Sciences. 2022;79:null.
27. Hermans F, Hasevoets S, Vankelecom H, Bronckaers A, Lambrichts I. From Pluripotent Stem Cells to Organoids and Bioprinting: Recent Advances in Dental Epithelium and Ameloblast Models to Study Tooth Biology and Regeneration. Stem Cell Rev Rep. 2024 Mar 18;
28. Hemeryck L, Lambrichts I, Bronckaers A, Vankelecom H. Establishing Organoids from Human Tooth as a Powerful Tool Toward Mechanistic Research and Regenerative Therapy. J Vis Exp. 2022 Apr 13;(182).
29. Hilkens P, Gervois P, Fanton Y, Vanormelingen J, Martens W, Struys T, et al. Effect of isolation methodology on stem cell properties and multilineage differentiation potential of human dental pulp stem cells. Cell Tissue Res. 2013 Jul 1;353(1):65–78.
30. Merckx G, Lo Monaco M, Lambrichts I, Himmelreich U, Bronckaers A, Wolfs E. Safety and Homing of Human Dental Pulp Stromal Cells in Head and Neck Cancer. Stem Cell Rev and Rep. 2021 Oct 1;17(5):1619–34.
31. Zhang Z, Warner KA, Mantesso A, Nör JE. PDGF-BB signaling via PDGFR-β regulates the maturation of blood vessels generated upon vasculogenic differentiation of dental pulp stem cells. Front Cell Dev Biol [Internet]. 2022 Oct 19 [cited 2024 Aug 9];10. Available from: https://www.frontiersin.org/journals/cell-and-developmental-biology/articles/10.3389/fcell.2022.977725/full
32. Carpentier G, Berndt S, Ferratge S, Rasband W, Cuendet M, Uzan G, et al. Angiogenesis Analyzer for ImageJ — A comparative morphometric analysis of "Endothelial Tube Formation Assay" and "Fibrin Bead Assay." Sci Rep. 2020 Jul 14;10(1):11568.
33. Remmers SJA, van der Heijden FC, Ito K, Hofmann S. The effects of seeding density and osteoclastic supplement concentration on osteoclastic differentiation and resorption. Bone Reports. 2023 Jun 1;18:101651.
34. Ferrara N, Gerber HP, LeCouter J. The biology of VEGF and its receptors. Nat Med. 2003 Jun;9(6):669–76.
35. Goncharov NV, Popova PI, Avdonin PP, Kudryavtsev IV, Serebryakova MK, Korf EA, et al. Markers of Endothelial Cells in Normal and Pathological Conditions. Biochem (Mosc) Suppl Ser A Membr Cell Biol. 2020;14(3):167–83.

36. Nam H, Kim JW, Park J, Park JC, Kim JW, Seo B, et al. Expression profile of the stem cell markers in human Hertwig's epithelial root sheath/Epithelial rests of Malassez cells. Molecules and Cells. 2011;31:355–60.
37. Jiang W, Xu T, Song Z, Wang X, Yuan S, Li Q, et al. CCL2 is a key regulator and therapeutic target for periodontitis. J Clin Periodontol. 2023 Dec;50(12):1644–57.
38. Khan UA, Hashimi SM, Bakr MM, Forwood MR, Morrison NA. CCL2 and CCR2 are Essential for the Formation of Osteoclasts and Foreign Body Giant Cells. J Cell Biochem. 2016 Feb;117(2):382–9.
39. She S, Ren L, Chen P, Wang M, Chen D, Wang Y, et al. Functional Roles of Chemokine Receptor CCR2 and Its Ligands in Liver Disease. Front Immunol. 2022 Feb 25;13:812431.
40. Tsou CL, Peters W, Si Y, Slaymaker S, Aslanian AM, Weisberg SP, et al. Critical roles for CCR2 and MCP-3 in monocyte mobilization from bone marrow and recruitment to inflammatory sites. J Clin Invest. 2007 Apr 2;117(4):902–9.
41. Ades EW, Candal FJ, Swerlick RA, George VG, Summers S, Bosse DC, et al. HMEC-1: establishment of an immortalized human microvascular endothelial cell line. J Invest Dermatol. 1992 Dec;99(6):683–90.
42. Prigozhina NL, Heisel A, Wei K, Noberini R, Hunter EA, Calzolari D, et al. Characterization of a novel angiogenic model based on stable, fluorescently labeled endothelial cell lines amenable to scale-up for high content screening. Biol Cell. 2011 Oct 1;103(10):467–81.
43. Boyle WJ, Simonet WS, Lacey DL. Osteoclast differentiation and activation. Nature. 2003 May;423(6937):337–42.
44. Beekhuizen H, van Furth R. Monocyte adherence to human vascular endothelium. Journal of Leukocyte Biology. 1993 Oct 1;54(4):363–78.
45. Regulation of human monocyte adherence by granulocyte-macrophage colony-stimulating factor. [Internet]. [cited 2025 Jun 1]. Available from: https://www.pnas.org/doi/epdf/10.1073/pnas.86.18.7169
46. Mochizuki A, Takami M, Miyamoto Y, Nakamaki T, Tomoyasu S, Kadono Y, et al. Cell Adhesion Signaling Regulates RANK Expression in Osteoclast Precursors. PLOS ONE. 2012 Nov 6;7(11):e48795.
47. Takegahara N, Kim H, Choi Y. Unraveling the intricacies of osteoclast differentiation and maturation: insight into novel therapeutic strategies for bone-destructive diseases. Exp Mol Med. 2024 Feb;56(2):264–72.
48. Chandrabalan S, Dang L, Hansen U, Timmen M, Wehmeyer C, Stange R, et al. A novel method to efficiently differentiate human osteoclasts from blood-derived monocytes. Biological Procedures Online. 2024 Mar 19;26.
49. Boissy P, Saltel F, Bouniol C, Jurdic P, Machuca-Gayet I. Transcriptional Activity of Nuclei in Multinucleated Osteoclasts and Its Modulation by Calcitonin. Endocrinology. 2002 May 1;143(5):1913–21.
50. Simons M, Gordon E, Claesson-Welsh L. Mechanisms and regulation of endothelial VEGF receptor signalling. Nat Rev Mol Cell Biol. 2016 Oct;17(10):611–25.
51. Lee S, Chen TT, Barber CL, Jordan MC, Murdock J, Desai S, et al. Autocrine VEGF Signaling Is Required for Vascular Homeostasis. Cell. 2007 Aug 24;130(4):691–703.
52. Duffy AM, Bouchier-Hayes DJ, Harmey JH. Vascular Endothelial Growth Factor (VEGF) and Its Role in Non-Endothelial Cells: Autocrine Signalling by VEGF. In: Madame Curie Bioscience Database [Internet] [Internet]. Landes Bioscience; 2013 [cited 2025 May 20]. Available from: https://www.ncbi.nlm.nih.gov/books/NBK6482/
53. Matsui Y, Amano H, Ito Y, Eshima K, Tamaki H, Ogawa F, et al. The role of vascular endothelial growth factor receptor-1 signaling in compensatory contralateral lung growth following unilateral pneumonectomy. Lab Invest. 2015 May;95(5):456–68.
54. Bergamo MT, Zhang Z, Oliveira TM, Nör JE. VEGFR1 primes a unique cohort of dental pulp

stem cells for vasculogenic differentiation. Eur Cell Mater. 2021 Mar 16;41:332–44.
55. Weber KSC, Nelson PJ, Gröne HJ, Weber C. Expression of CCR2 by Endothelial Cells. Arteriosclerosis, Thrombosis, and Vascular Biology. 1999 Sep;19(9):2085–93.
56. Si Y, Tsou CL, Croft K, Charo IF. CCR2 mediates hematopoietic stem and progenitor cell trafficking to sites of inflammation in mice. J Clin Invest. 2010 Apr 1;120(4):1192–203.
57. Xu R, Ni B, Wang L, Shan J, Pan L, He Y, et al. CCR2-overexpressing mesenchymal stem cells targeting damaged liver enhance recovery of acute liver failure. Stem Cell Research & Therapy. 2022 Feb 5;13(1):55.
58. Peng Z, Pang H, Wu H, Peng X, Tan Q, Lin S, et al. CCL2 promotes proliferation, migration and angiogenesis through the MAPK/ERK1/2/MMP9, PI3K/AKT, Wnt/β-catenin signaling pathways in HUVECs. Exp Ther Med. 2022 Dec 27;25(2):77.
59. Möckel D, Bartneck M, Niemietz P, Wagner M, Ehling J, Rama E, et al. CCL2 chemokine inhibition primes the tumor vasculature for improved nanomedicine delivery and efficacy. Journal of Controlled Release. 2024 Jan 1;365:358–68.
60. Hayashi JN, Ito H, Kanayasu T, Asuwa N, Morita I, Ishii T, et al. Effects of glucose on migration, proliferation and tube formation by vascular endothelial cells. Virchows Archiv B Cell Pathol. 1991 Dec 1;60(1):245–52.
61. Ladaigue S, Paget V, Lefranc AC, Quitoco M, Bacquer E, Milliat F, et al. Protocol for *in vitro* assessment of human monocyte transendothelial migration using a high-throughput live cell imaging system. STAR Protocols. 2023 Sep 15;4(3):102388.
62. Ariffin SHZ, Wahab RMA, Razak MA, Yazid MD, Shahidan MA, Miskon A, et al. Evaluation of in vitro osteoblast and osteoclast differentiation from stem cell: a systematic review of morphological assays and staining techniques. PeerJ. 2024 Jul 25;12:e17790.
63. Human Osteoclast Culture From Peripheral Blood Monocytes | SpringerLink [Internet]. [cited 2025 Jun 5]. Available from: https://link-springer-com.bib-proxy.uhasselt.be/protocol/10.1385/1-59259-861-7:055
64. Hulley PA, Knowles HJ. A New Method to Sort Differentiating Osteoclasts into Defined Homogeneous Subgroups. Cells. 2022 Jan;11(24):3973.
65. Lv G, Heinemann C, Wiesmann HP, Kruppke B. Artificial Intelligence for Image-Based Identification of Osteoclasts and Assessment of Their Maturation—Using the OC_Identifier. Applied Sciences. 2025 Jan;15(8):4159.

Acknowledgements **– I would like to thank my supervisor, Dr. Florian Hermans, for his strong support and valuable guidance throughout this project. I am also grateful to my principal investigator, Prof. Dr. Ivo Lambrichts, for providing access to the microscopy facilities. Sincere thanks to Prof. Dr. Annelies Bronckaers, Prof. Dr. Ivo Lambrichts, and the entire team for their constructive feedback and advice during my internship. A special thanks to lab technicians Evelyne Van Kerckhove, Ellen SLEURS, and Petra Bex for their technical assistance and support. OpenAI was used to improve the clarity of the text and assist in identifying relevant research sources.**

Author contributions – Dr. Florian Hermans conceived and designed the research. Steffie Hasevoets cultured the tooth organoid and collected the conditioned medium. Dr. Pieter Ruytinx performed and designed osteoclast experiments. Mai Hoang Ngoc Phuong performed experiments, contributed to the experimental design, and carried out data analysis and report writing. Prof. Dr. Ivo Lambrichts and Dr. Florian Hermans provided critical feedback on the report.

SUPPLEMENTARY

Table S2 – Tooth organoid medium (TOM) composition

Product	Concentration	Supplier	Product
Serum-free defined medium (SFDM)	See Table 2 for composition	Thermo Fisher Scientific	Serum-free defined medium (SFDM)
A83-01	0.5 µM	Sigma-Aldrich	A83-01
B27 (without vitamin A)	2%	Gibco	B27 (without vitamin A)
Cholera Toxin	100 ng/mL	Sigma-Aldrich	Cholera Toxin
FGF2 (= basic FGF)	20 ng/mL	R&D Systems	FGF2 (= basic FGF)
FGF8	200 ng/mL	Peprotech	FGF8
FGF10	100 ng/mL	Peprotech	FGF10
L-Glutamine	2 mM	Gibco	L-Glutamine
IGF-1	100 ng/mL	Peprotech	IGF-1
N2	1%	Gibco	N2
N-acetyl L-cysteine	1.25 mM	Sigma-Aldrich	N-acetyl L-cysteine
Nicotinamide	10 mM	Sigma-Aldrich	Nicotinamide

Table S2 – Serum-free defined medium (SFDM; pH 7.3) composition

Product	Concentration	Supplier
Sterile H2O		
DMEM 1:1 F12 without Fe	16.8 g/L	Invitrogen
Transferrin	5 mg/L	Serva
Insulin from bovine pancreas	5 mg/L	Sigma-Aldrich
Penicillin G sodium salt	35 mg/L	Sigma-Aldrich
Streptomycin sulfate salt	50 mg/L	Sigma-Aldrich
Ethanol absolute, ≥99.8% (EtOH)	600 µL/L	Fisher Chemical
Catalase from bovine liver	50 µL/L	Sigma-Aldrich
IGF-1	100 ng/mL	Peprotech
N2	1%	Gibco
N-acetyl L-cysteine	1.25 mM	Sigma-Aldrich
Nicotinamide	10 mM	Sigma-Aldrich

Table S3 – Glucose measurement of different healthy donor derived ERM-TO CM for normalization

Sample	Value
P51	71 mg/dl
P52	27 mg/dl
P53	74 mg/dl
P54	74 mg/dl
P55	78 mg/dl
P56	29 mg/dl
P66	56 mg/dl
P67	24 mg/dl
P69	50 mg/dl
P70	44 mg/dl
P72	48 mg/dl
P73	32 mg/dl
Blank	—

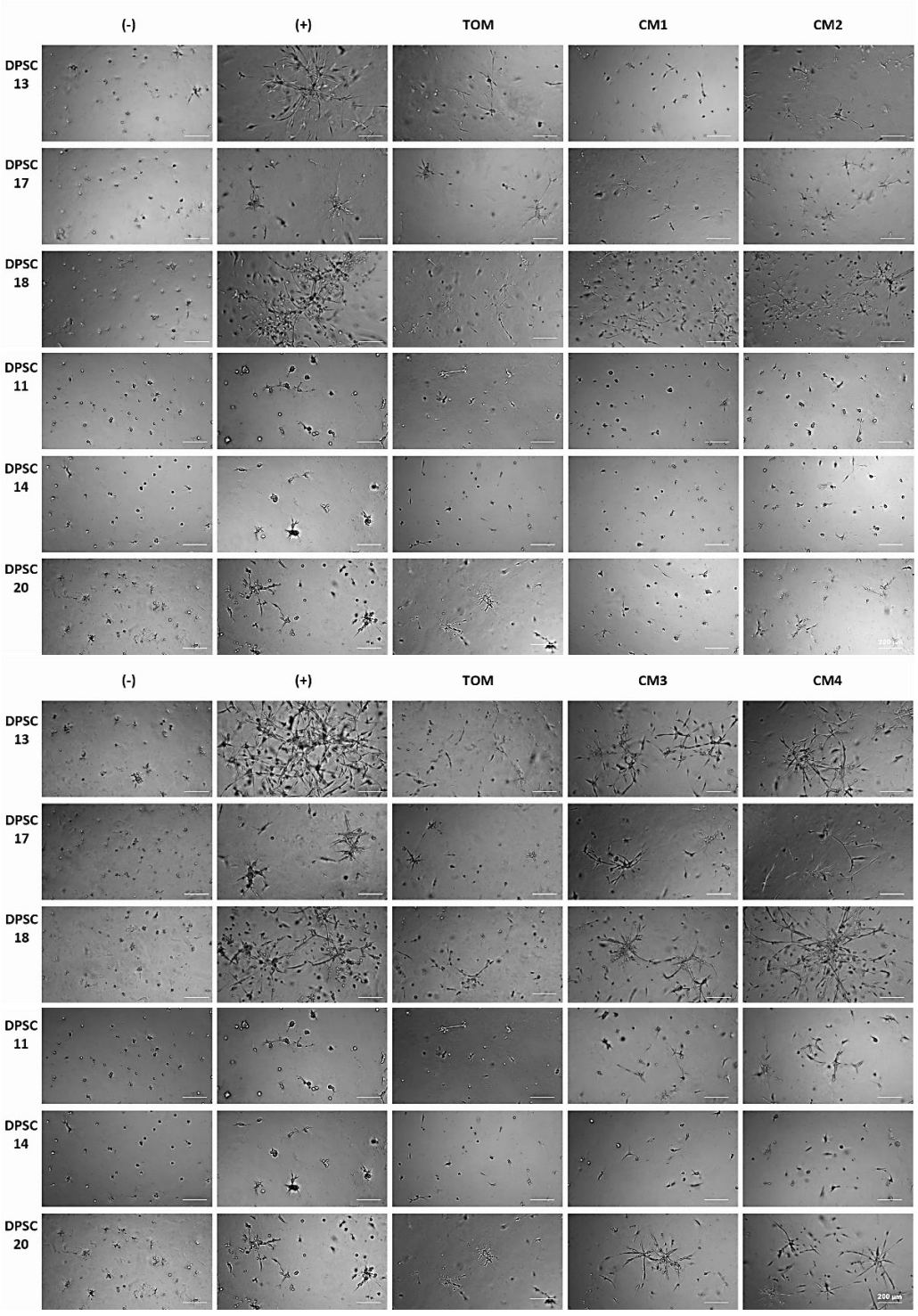

Fig. S1 – ERM-TO CM effect on endothelial cell differentiation of different patient's DPSCs. (-): negative control, (+): positive control, TOM: tooth organoid medium, CMs: ERM-TO CM diluted in (-) medium for glucose normalization (n=6).

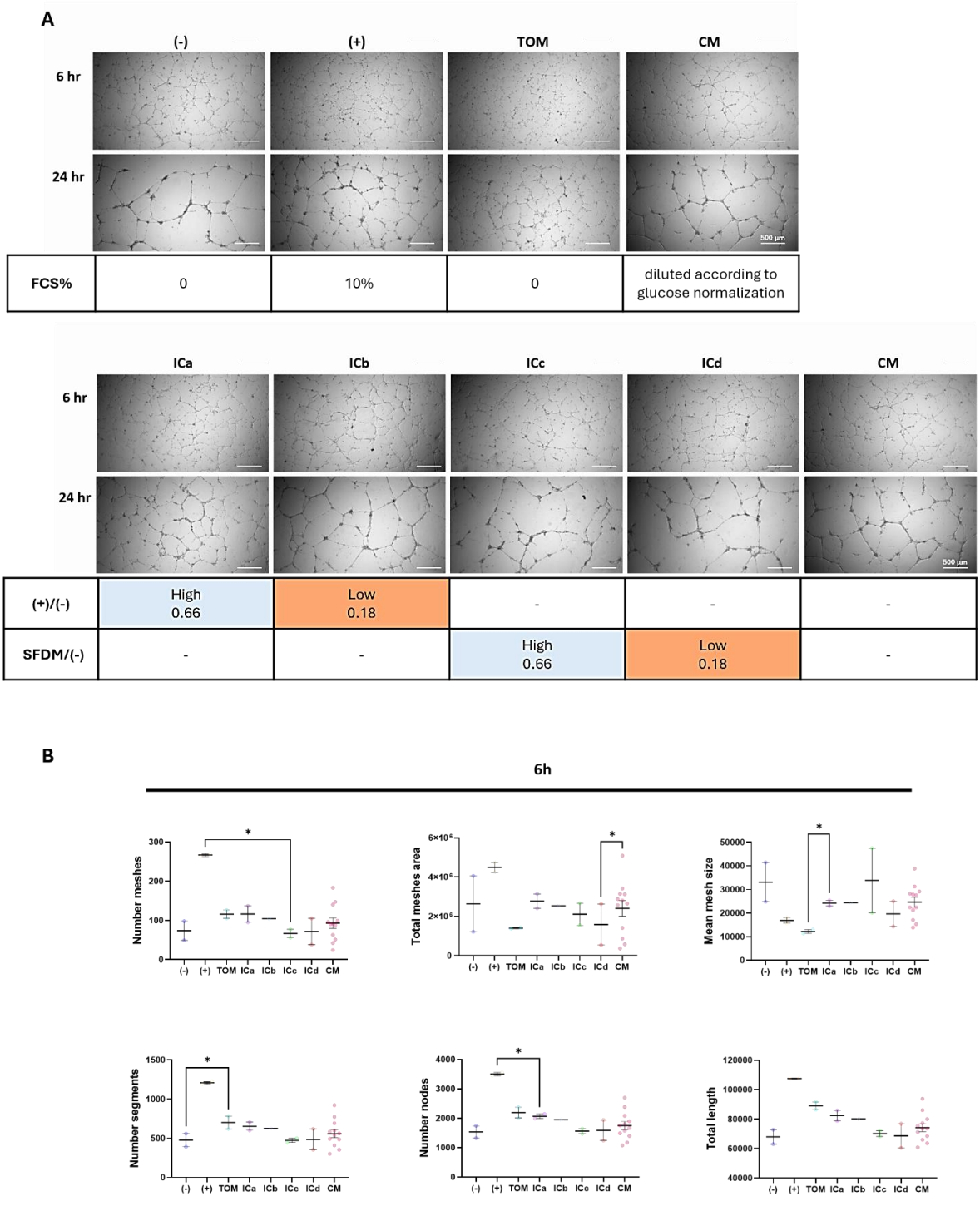

Fig. S2 – **ERM-TO CM effect on tube formation of HMEC-1.** (A) HMEC-1 tube formation in control conditions, internal control conditions for omitting the effect of TOM (ICa&b) and serum dilution (ICc&d) on tube formation, and ERM-TO CMs. (-): negative control, (+): positive control, TOM: tooth organoid medium, ICa: internal control 'a', ICb: internal control 'b', ICc: internal control 'c', ICd: internal control 'd', CM: ERM-TO CM diluted in (-) medium for glucose normalization (n=1). (B) Quantification of tube formation result at 6h.

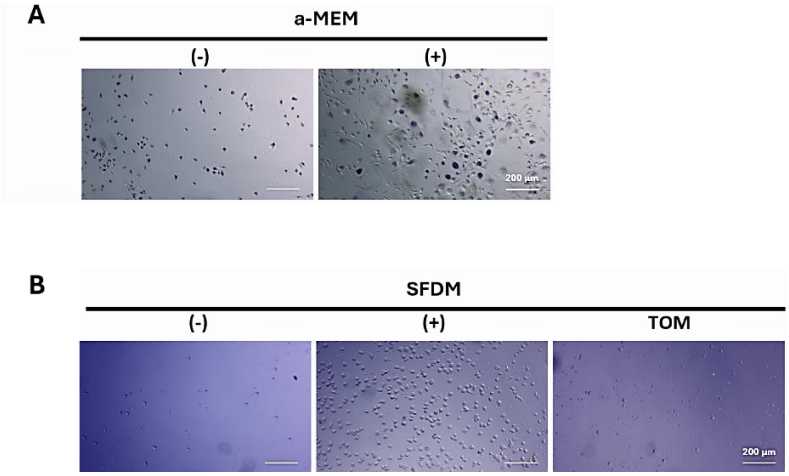

Fig. S3 – Optimization of osteoclast differentiation from PBMCs under a-MEM and SFDM based medium. (A) TRAP staining on day 7 demonstrated successful osteoclast differentiation in cultures maintained in α-MEM-based medium. Mature, multinucleated osteoclasts were clearly observed. (B) TRAP staining of osteoclast differentiated under SFDM based medium on D7 showed no osteoclasts formed. (-): negative control, medium supplemented with 1% P/S, and 10% FCS, (+) positive control, medium supplemented with 1% P/S, 10% FCS, 1 ng/mL TGF-B1, 30 ng/mL M-CSF, 10 ng/mL RANKL, TOM: Tooth organoid medium (n=2).

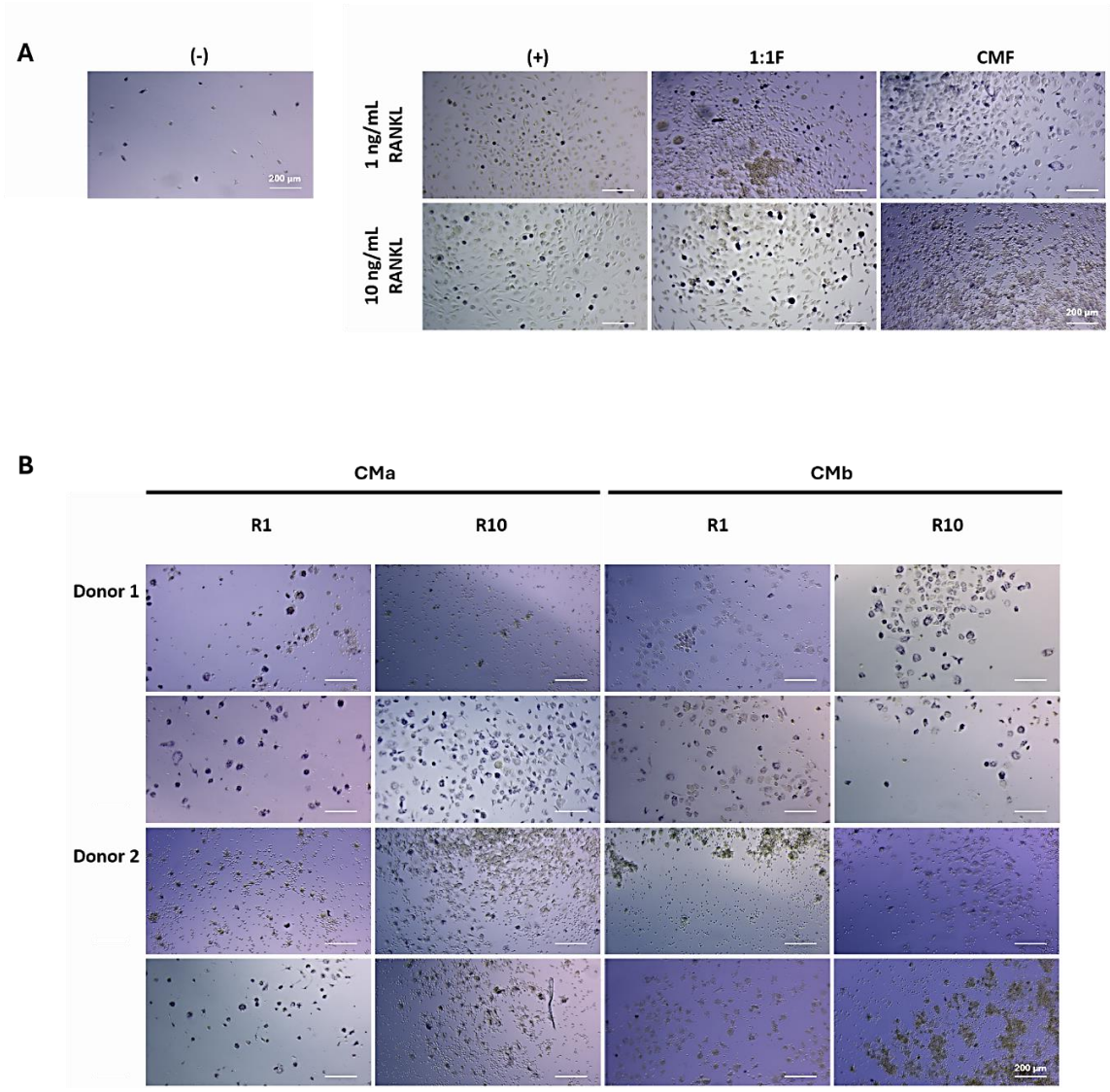

Fig. S4 – **ERM-TO CM effect on osteoclast differentiation from PBMCs.** (A) Optimization of osteoclast differentiating under ERM-TO CM with addition of FCS. (-) negative control, (b) positive control with addition of 1 ng/mL TGF-B1, 30 ng/mL M-CSF, 1 ng/mL or 10 ng/mL RANK, (CMFs) ERM-TO CMs diluted in (-) with 1:1 ratio and supplemented with 10%FCS, 1 ng/mL TGF-B1, 30 ng/mL M-CSF, 1 ng/mL or 10 ng/mL RANKL (B) Variance of osteoclast differentiated under ERM-TO CM (n=2). CMa: ERM-TO CMs diluted in (-) with 1:1 ratio and supplemented with 1 ng/mL TGF-B1, 30 ng/mL M-CSF, 1 ng/mL or 10 ng/mL RANKL